Iraqi Journal of Physics, 2019 *Vol.17, No.42, PP. 108-124*

DOI: 10.20723/ijp.17.42.108-124

Characterization of zinc oxide nanostructures prepared by hydrothermal method with antibacterial property

Ibrahim A. Ali and Sabah H. Sabeeh

Applied Physics Department, University of Technology, Baghdad, Iraq

E-mail: sabahhabeeb@gmail.com

Abstract

In this research, zinc oxide nanostructures were prepared via hydrothermal method utilized two compounds, zinc nitrate hexahydrate and sodium hydroxide consider as a precursor. Three annealing temperatures were used to study their effect on ZnO nanostructures properties. The synthesized nanostructure was described utilizing x-ray diffraction (XRD), Field Emission Scanning Electron Microscopy (FESEM), Atomic Force Microscope (AFM), and Fourier Transform Infrared Spectroscopy (FTIR). Optical characterization was studied utilized UV -visible spectroscopy. XRD analysis confirms that all ZnO nanostructures have the hexagonal wurtzite structure with average crystallite size within the range of (30.59-34.52) nm. The crystallite size increases due to the incensement of annealing temperature. FESEM analysis indicates that ZnO has hexagonal shape of cylindrical pores, plate-like nanocrystals and Nanorods. AFM analysis shows that the average surface roughness of ZnO nanostructures increases from 3.96 to 19.1 nm with the increase of annealing temperature. The FTIR peaks indicate successful preparation of ZnO nanostructures. The FTIR method was used to analyses the chemical bonds which conformed the present of the Zn-O group in the region between (400-500) cm^{-1}. UV-visible analysis appears red shift in absorption spectra due to shifting in energy gap with increment of particle size. The band gap energy has been calculated from the optical absorption spectra. The annealing process has been found more effective on the value of energy gap. As the annealing temperature increases, the value of energy gap, increases as well; from (3.12 to 3.22) eV. The prepared nanostructure is used for antibacterial property shows strong activity against S. aureus bacteria, P.aeuruginosa bacteria by disc diffusion test (agar method test). White precipitate of ZnO nanostructures has superior antibacterial activity towards gram-positive (S. aureus) bacteria than gram-negative (P.aeuruginosa) bacteria.

Key words

ZnO nanostructure, hydrothermal method, annealing temperature, antibacterial activity.

Article info.

Received: May. 2019
Accepted: Jun. 2019
Published: Sep. 2019

خصائص اوكسيد الخارصين ذو التركيب النانوي المحضر بطريقة الحرارية المائية مع خاصية المضاد للبكتيريا

ابراهيم عبد الكريم علي و صباح حبيب صبيح

قسم العلوم التطبيقية، الجامعة التكنولوجية، بغداد، العراق

الخلاصة

في هذا البحث تم تحضير اوكسيد الخارصين النانوي بطريقة الحرارية المائية باستخدام نترات الخارصين المهدرجة و هيدروكسيد الصوديوم كباديء للتفاعل. تم استخدام ثلاث درجات حرارية مختلفة لدراسة تاثيرها على خصائص اوكسيد الخارصين ذو التركيب النانوي. لفحص خواص التركيب النانوي المحضر نستخدام حيود الاشعة السينية و والمجهر الالكتروني الماسح ومجهر القوى الذري وتحويلة فورير للاشعة تحت الحمراء. تم الكشف عن الخصائص البصرية وتحليلها باستخدام مطياف الاشعة الفوق البنفسجية. اكدت نتائج فحص جهاز حيود الاشعة السينية تكون اوكسيد الخارصين ذو التركيب السداسي (الورتزايت) وان معدل الحجم الحبيبي يتراوح بين (34.52-59.30) نانومتر. كما ان الحجم الحبيبي يزداد بزيادة درجه حرارة التلدين. اكدت نتائج المجهر الالكتروني الماسح ان اوكسيد الخارصين يمتلك تركيب سداسي على شكل مسام اسطواني، صفائح من البلورات الناوية، عود نانوي. اكدت نتائج فحص مجهر القوى الذري بان معدل خشونة السطح لاوكسيد الخارصين النانوي يزداد بزيادة درجة حرارة التلدين. تم استخدام تحويله فورير للاشعة تحت الحمراء للكشف عن الاواصر الكيميائية التي اكدت على وجود مجموعة اوكسيد الخارصين (خارصين – اوكسجين) في المنطقه ما بين (400-500) cm^{-1}. لاحظت نتائج فحص مطياف الاشعة الفوق البنفسجية وجود ازاحة حمراء في طيف الامتصاص يعود الى الازاحة الحاصلة في فجوة الطاقة نتيجة الزيادة في الحجم الحبيبي. تم حساب فجوة الطاقة بلاعتماد على طيف الامتصاص البصري. وجد ان طريقة التلدين اكثر كفائة وتاثيرا على قيمة فجوة الطاقة. لاحظ بزيادة درجة حرارة التلدين مقدار فجوة الطاقة يقل من (3.22- 3.12) الكترون- فولت. مقدار فجوة الطاقة يزداد بزيادة تركيز هيدروكسيد الصوديوم من (3.27-3.36) الكترون- فولت. تم استخدام اوكسيد الخارصين النانوي كمضاد للبكتريا. اظهر اوكسيد الخارصين النانوي نشاط قوي مضاد للبكتريا ضد بكتريا (S. aureus) و بكتريا (P.aeuruginosa)استخدام طريقة نظام نشرالقرص. وجد ان اوكسيد الخارصين النانوي يمتلك نشاط مضاد للبكتريا فائق ضد بكتريا غرام- موجب (S. aureus) اكثر من بكتريا غرام سالب (P.aeuruginosa).

Introduction

Zinc oxide nanostructures took awareness in modern materials science due to its properties [1]. ZnO has wide band gap (3.37 eV), higher melting point (2248 k), large excitation binding energy (60 meV), ZnO NSs having hexagonal structure Wurtzite with lattice spacing constants (a = 0.325nm) and (c = 0.521 nm) [2] and has been widely used in many applications such as gas sensors, transparent conductive films, varistors, efficient photo catalysts, electrical and optical devices and antibacterial application [3-6]. Many different methods are used to synthesizes it; such as pulsed laser deposition (PLD) [7], sputtering [8], sol-gel [9], and metal organic chemical vapor deposition (MOCVD) [10] hydrothermal synthesis [11] etc. Among these methods, the hydrothermal method is more popular because of its simplicity, inexpensive, accuracy and repeatability. The nanostructures which are prepared by using this route show good optical properties by monitoring the size and morphology of the particles in addition to having control on hydrothermal process and the growth of nuclei [12]. Physically zinc oxide nanoparticles exist in white powder form and exhibit an electric property of n-type conductive while its p-type conductivity may obtained by special synthesis process. In addition, researchers study antimicrobial activity of ZnO NSs against bacteria Gram-negative including Pseudomonas aeruginosa, Escherichia coli, campylobacter jejuni, and bacteria Gram-positive such Bacillus subtillis and Staphylococcus aureus [13]. It's the first time we synthesis ZnO NSs utilized the molarity 2.5 M NaOH concentrations and 0.2M Zinc nitrate hexahydrate by hydrothermal method. The growth is carried out in 150 °C. Cost is minimal due to use simpler equipment and cheaper chemicals. Our study is an attempt discussing amends of the annealing temperatures for obtained particle size requirements and shape to turn it suitable for biomedical application. ZnO nanostructures exhibit varying different morphologies (nano plate, nanorods, and cylindrical

pores) with respect to the annealing temperatures. Optical characterizations of ZnO nanostructures have good transmittance in the visible region. ZnO nanostructures produced good antibacterial activities when grain size decreased to nanometer range. ZnO enters inside the cell due to interactions with bacterial surface and/or with bacterial core, subsequently described distinct bactericidal mechanism. The aim of our work is to produce better antibacterial agent by using constant concentration of fine ZnO NSs (25µl) having small size. Our study showed higher antibacterial activities to gram bacteria positive (S. aureus) than the gram-negative bacteria (P.aeuruginosa) and the analysis obtained inhibition efficacy of ZnO nanostructures strongly dependent on concentration and size.

Materials and methods

1- Preparation of ZnO nanostructure

ZnO nanostructure was prepared via hydrothermal growth by utilized zinc nitrate hexahydrate, sodium hydroxide as precursors. All materials were used as received from Thomas Baker chemicals, India. Zinc nitrate hexahydrate [Zn $(NO_3)_2.6H_2O$] (0.2 M) dissolved in (50 ml) deionized water put down in beaker at room temperature, with continues stirring for (5 min). Sodium hydroxide NaOH (2.5 M) was dissolved in deionized water of 25 ml in separate beaker under continues stirring for (5 min). After that, aqueous solution of sodium hydroxide was applied to Zinc nitrate hexahydrate aqueous solution under stirring condition. White aqueous solution was obtained and then inserted in a Teflon lined-stainless autoclave and put into an electrical oven at 150 °C for 6 hours. The reactor was naturally cooled at room temperature. These solutions were reacted to produce zinc hydroxide Zn $(OH)_2$. Following the precipitation, the solution was centrifuged at 3000 rpm for (30 min), after that washed utilized distilled water and alcohol (C_2H_5OH) many times. Put aqueous solution in electrical oven at 80 °C for 4 hours. The result had been white precipitation of ZnO. The chemical reactions were observed for this hydrothermal synthesis is as follow:

$$Zn(NO_3)_2.6H_2O + 2NaOH \rightarrow Zn(OH)_2 + 2NaNO_3 + 6H_2O$$

$$Zn(OH)_2 \rightarrow ZnO + H_2O$$

2- Characterizations of ZnO

The crystallinity and phases of the ZnO were investigated by utilizing X-ray diffractometer, by (Lab X, XRD-6000 Shimazdu). X-ray diffraction analysis achieved and matched according to the standard (JCPDS Card no: 00-036-1451). The crystal size was calculated by using Scherer -Debye Equation.

Field Emission Scanning Electron Microscope device type (TESCAN MIRA3 FE-SEM) was used to visualize very small topographic information on the surface of fractioned or entire of the sample.

In this work Atomic Force Microscope (CSPM-AA3000), AFM was utilized as an instrument to measure the granularity accumulation distribution, roughness, and grain size of the ZnO nanoparticles. In this test three dimensional images of the surface of the ZnO nanostructure are obtained.

[FTIR] (SHIMADZU IRAFFINITY) includes interaction of infrared radiation with metal oxide (matter) that mostly established on absorption spectroscopy. The analysis of the FTIR is completed over the range between (400–4000) cm^{-1}.

Optical properties were studied and calculate the energy gap at different annealing temperatures, absorption. UV-Visible spectrophotometer has been used in the wavelength range (370-720 nm). (UV-VIS-1650) type PC Shimadzu ultraviolet spectrophotometer-Japan was utilized to characterized the optical absorption. For antibacterial activity test 5mg of ZnO nanostructures was dissolved in 5ml dimethyl sulfoxide DMSO and thus absorption spectra has been recorded.

The Antibacterial activity of zinc oxide nanostructures on gram positive (S.aurous) and gram-negative (Aeruginosa) bacteria tested by utilized agar diffusion method [14]. ZnO Nano powders were antiseptic before applied to the disk, still in an autoclave for (15 min) at 120 °C. The grown was executed on nutrient agar media for both Bactria at 37 °C for (24 hour). Nutrient agar media was prepared utilized diluting 28g powder of nutrient agar in 1000ml distilled water. Subsequently, aqueous solution was sterilized in an autoclave for (20 min) and drain in sterile petri dishes. The bacterial count had set up according to McFarland aqueous solution (0.5) by normal saline. 1 mg of each ZnO NSs was diluted in 5 ml of dimethyl sulfoxide (DMSO) using magnetic stirrer for 15 minutes obtained aqueous suspensions of ZnO NSs. 25µl of DMSO was loaded onto filter paper discs that utilized as control zone for both control positive and control negative. 25 µl of sterile aqueous suspensions of ZnO were transferred and spread into an antiseptic standard filter paper discs that have diameter of (5 mm) placed into inoculated plates. Subsequently, plates were incubated at (37 °C) still inside for (24 hours). The inhibition zone could form around disc and measured in "millimeters" (mm) and then recorded.

Results and discussions

1- X-Ray diffraction

Fig.1 describes the XRD spectra of white precipitation ZnO Nanostructures prepared by hydrothermal growth. The diffraction peaks of this figure were closely corresponding to the peaks positions of JCPDS (No. 00-036-1451). diffraction peaks of Zinc oxide Nanostructures correspond to (100), (002), (101), (102), (110), (103), (200), (112), (201) and (202) planes that are located at 31.7214, 34.3803, 36.2051, 47.4905, 56.5435, 62.8042, 66.3217, 67.8930, 69.0333 and 76.9074 respectively. The result obtained indicates that the white precipitation of ZnO Nanopowder prepared at different conditions have a hexagonal wurtzite structure. Crystallite size (D) of ZnO equals to (30.59297) nm due to the high intensity peak (101). The lattice parameters was equal to (a=0.325176 nm and c= 0.520766 nm). The values are much closed as compared with the lattice constant of ZnO bulk in good agreement with previous work reports [15]. Fig.2 shows the XRD spectra of ZnO NSs annealed at different temperatures (300, 400 and 500) °C. The sharpness and relative intensities of the peaks tend to increase with increment of annealing temperature. Average crystallite size also increased with annealing temperatures reached to (34.52983) nm at 500 °C. The reaction temperature influences the structural morphology as well as the particle size. During annealing process, ZnO particles start formed, they collide and either coalesce with one another to form large particle or coagulate [16]. Table 1 shows the XRD analysis of ZnO Nanostructures prepared by using 2.5 M sodium hydroxide. The stress occurs in ZnO nanostructures show us the way to determining distortions that occur in crystal during the preparation step of the sample. The reason related

to exposure the sample to several factors such external strain, temperature, pressing and structural defects (oxygen vacancies and zinc/oxygen interstitials). The stress and strain was obtained and recorded as shown in Table 2. The strain increase when the lattice constant of the sample decreased. For 300 °C and 400 °C, the strain (ε<0) suggested ZnO NSs is subjected to compression stress. For 500 °C the stress becomes positive (ε>0) suggesting that the nanostructures is subjected to tensile stress.

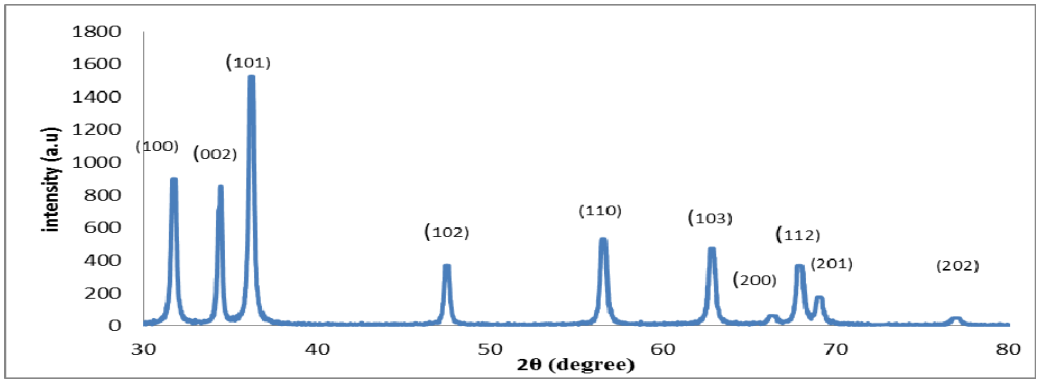

Fig. 1: XRD patterns of ZnO nanostructures synthesised using 2.5 M NaOH concentration by hydrothermal method.

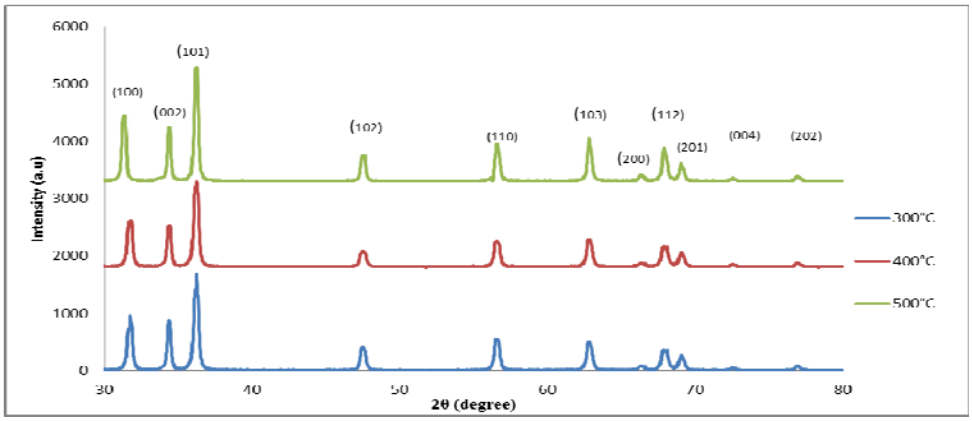

Fig.2: XRD patterns of ZnO nanostructures synthesised using 2.5 M sodium hydroxide concentration and annealed at (300 °C, 400 °C and 500 °C).

Table 1: The X-ray diffraction parameter and grain size of ZnO nanostructures prepared using 2.5 M NaOH.

Hkl	2θ (degree)	FWHM (degree)	Grain size (nm)
(100)	31.7214	0.27980	29.5167
(002)	34.3803	0.23570	35.28142
(101)	36.2051	0.27320	30.59297
(102)	47.4905	0.27870	31.14118
(110)	56.5435	0.29730	30.34077
(103)	62.8042	0.28370	32.72416
(200)	66.3217	0.27310	34.7488
(112)	67.8930	0.33780	28.34995
(201)	69.0333	0.33640	28.66107
(202)	76.9074	0.29600	34.27204

Table 2: Characteristics of the ZnO nanostructures obtained from XRD data.

Sample	d(Å) at (002)	d(Å) at(110)	a (Å)	c (Å)	e_{aa}	e_{cc}	$S_c(GNm^{-2})$
Without annealing	2.60638	1.62629	3.25258	5.21276	0.1181	0.0849	-531.536
300°C	2.60383	1.62588	3.25176	5.20766	0.0202	0.0597	-90.75
°C400	2.60762	1.62700	3.254	5.21524	0.1658	0.1286	-745.879
°C500	2.60152	1.62463	3.24926	5.20304	-0.069	-0.017	308.5501

2- Field-emission Scanning Electron Microscopy (FESEM)

Nano structural characterization of pure Zinc oxide was investigated by FESEM. Fig.3 shows FE-SEM images of ZnO NSs prepared with 2.5 M NaOH at different conditions. FESEM image of ZnO nanostructure were represented high magnifications of the surface in the range of (33.32 nm-55.76 nm). FE-SEM images of ZnO Nanostructures prepared with 2.5 M NaOH as seen in Fig.3 (A) was appeared irregular agglomerated of as prepared ZnO nanocrystals that include compressed cylindrical pores shaped [15]. The effect of annealing temperature showed plate-like nanocrystals of ZnO hexagonal structure as seen in Fig.3 (B). ZnO Nanorods were appeared in the Fig.3 (C) when reached the annealing temperature 400 ^{0}C, Fig.3 (D) shows irregular agglomerated of plate-like nanocrystals and Nanorods. The variation in size and shape of ZnO NSs were affected by annealing temperatures. This indicates that the growth of ZnO nanostructures increased with increasing the annealing temperatures. The obtained outcome is correspondence with previously reported [17].

3- Atomic Force Microscopy (AFM)

Fig.4 appears 2D and 3D AFM images of ZnO Nanostructures at various annealing temperatures (300, 400 and 500) °C. The grain size of ZnO Nanostructures and roughness substantially depend on the annealing temperature that leads to increase the surface roughness of ZnO NSs which results in denser particle structure due to enough diffusion activation energy of atoms that occupy site in crystal lattice and the grains becomes larger with lower surface energy that agrees with previous researches [18]. The images of ZnO Nanostructures appear uniform distributions onto the matrix and the grains have spherical nanostructures on the crystalline axis. Table 3 shows the AFM data includes the Roughness Average and root mean square roughness (RMS). The value of RMS roughness increased with increasing the annealing temperature reached to the maximum value 22.1 nm at 500°C as shown in Fig.5. The grain size observed from AFM analysis was greater than the grain size obtained from XRD, because the grains are accumulation of many crystals and the AFM measurements give the size of the grain while XRD obtained the size of crystals.Fig.5 shows the RMS roughness of ZnO nanostructures at different annealing temperatures.

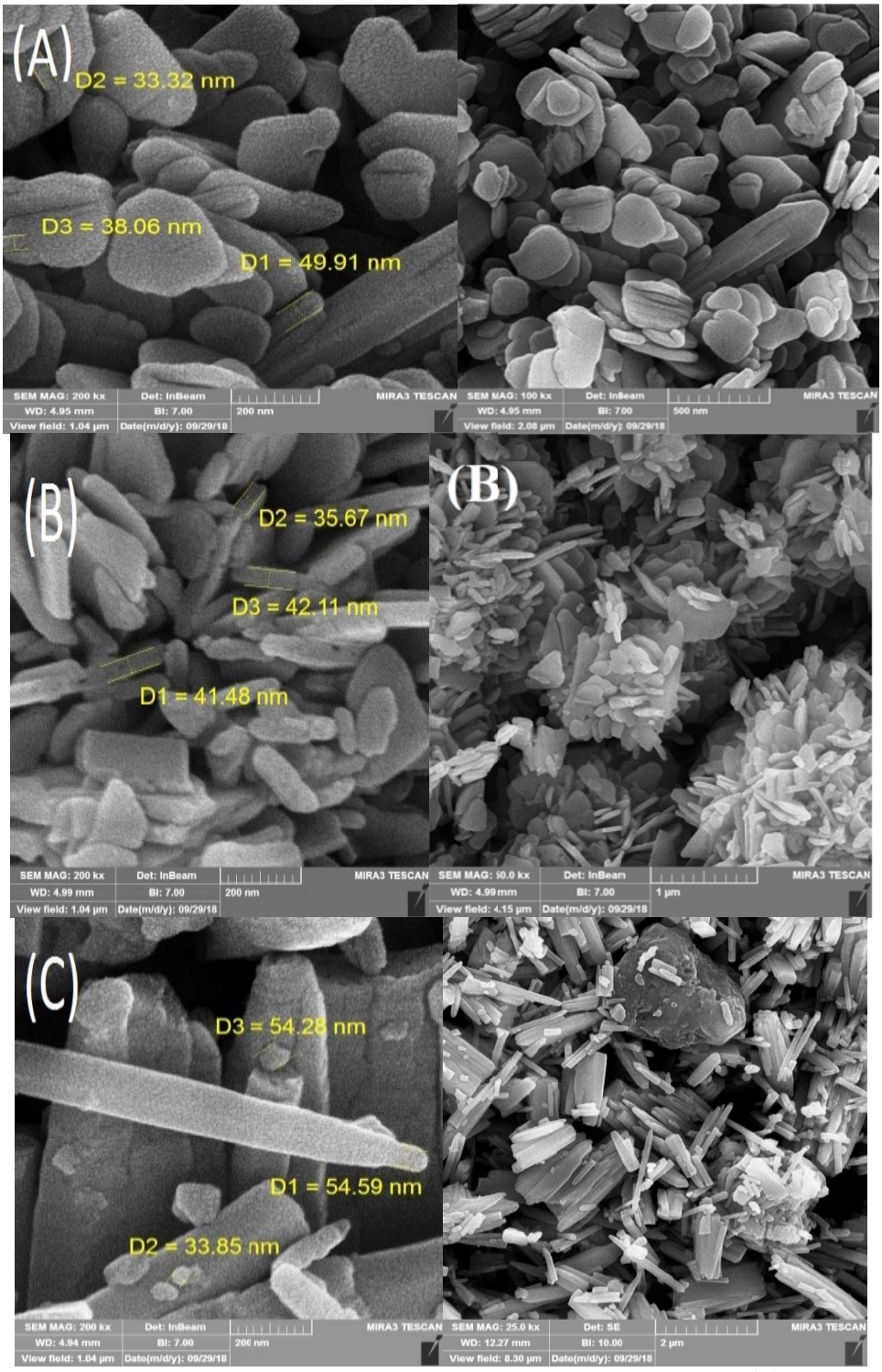

Fig.3: FE-SEM image of the ZnO nanostructures with 2.5 M NaOH at (A) As prepared (B) 300 °C, (C) 400 °C.

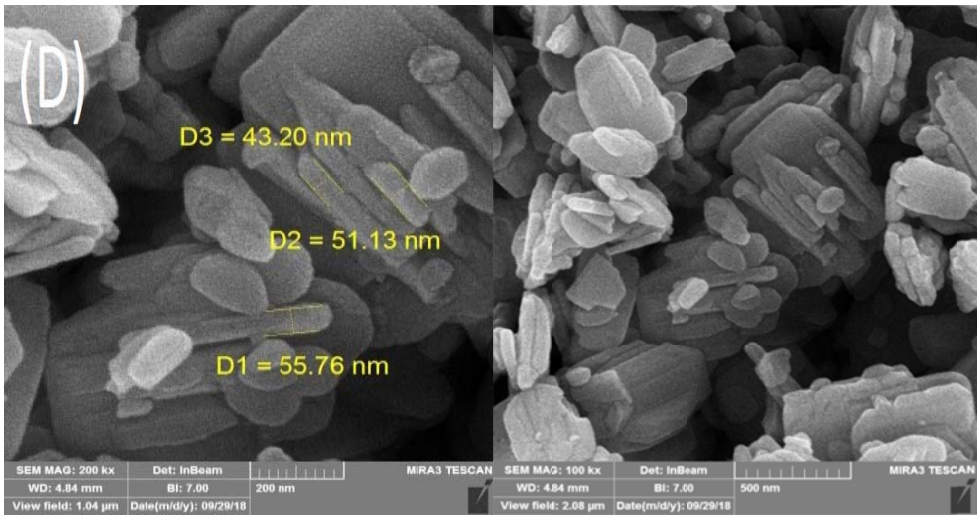

Fig.3: FE-SEM image of the ZnO nanostructures with 2.5 M NaOH at (D) 500 °C.

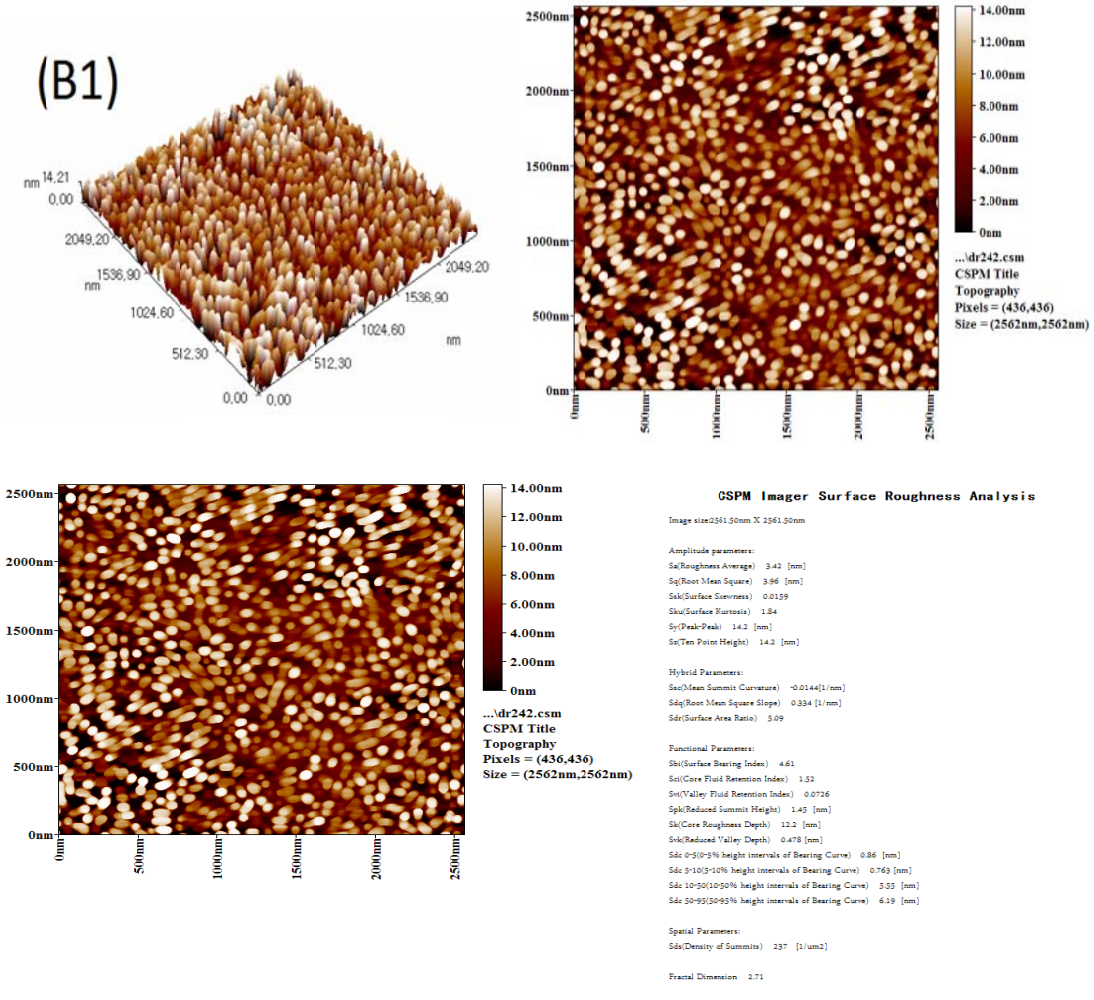

Fig.4: The 2D and 3D AFM images of the ZnO nanostructures at various annealing temperatures (300, 400 and 500) °C.

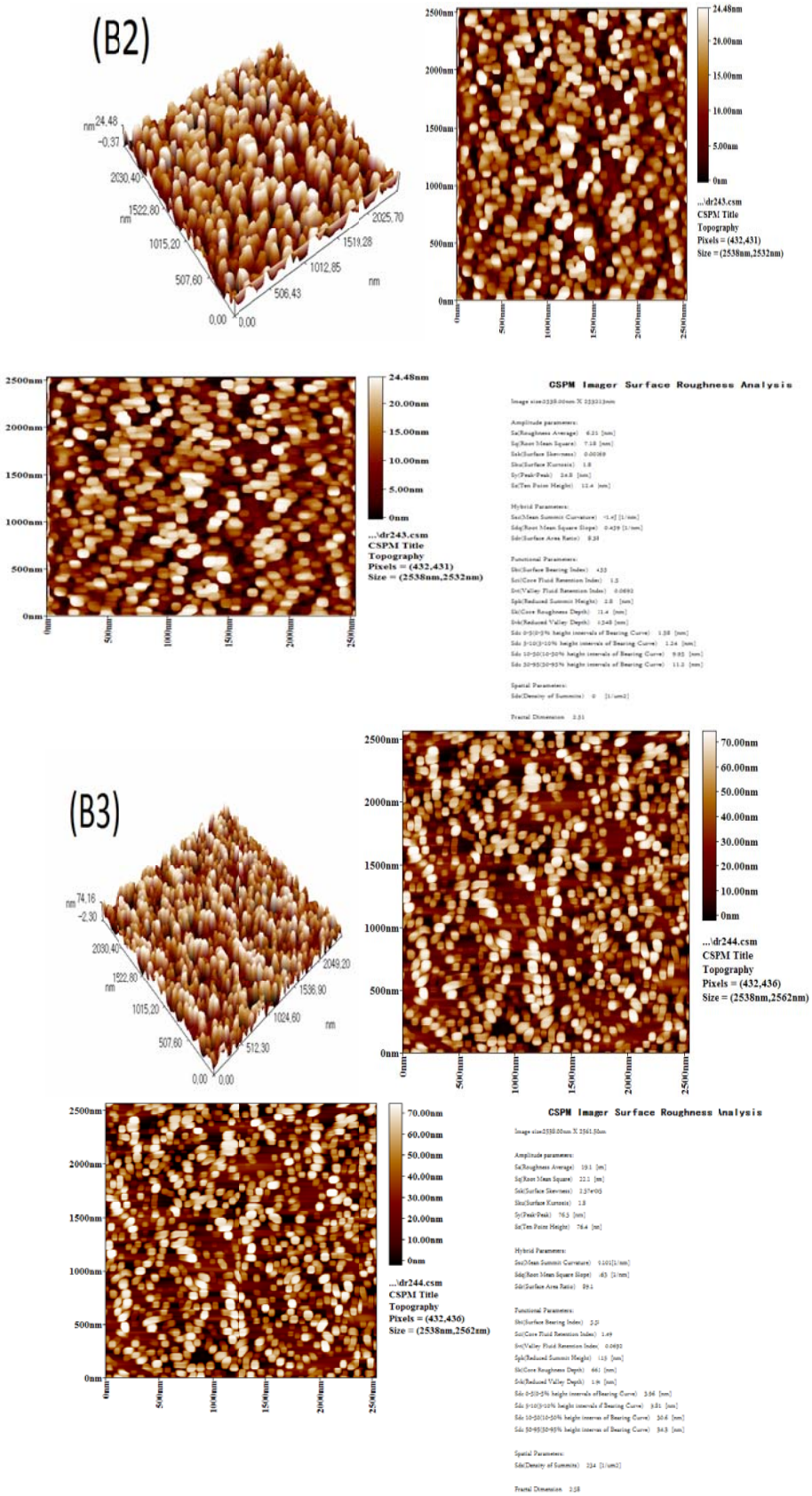

Fig.4: The 2D and 3D AFM images of the ZnO nanostructures at various annealing temperatures (300, 400 and 500) °C.

Table 3: The AFM data of ZnO nanostructure.

Annealing temperature	D(nm)	Roughness Average (nm)	RMS roughness (nm)
300 °C	75.44	3.96	3.42
400 °C	91.80	7.18	6.21
500 °C	67.66	19.1	22.1

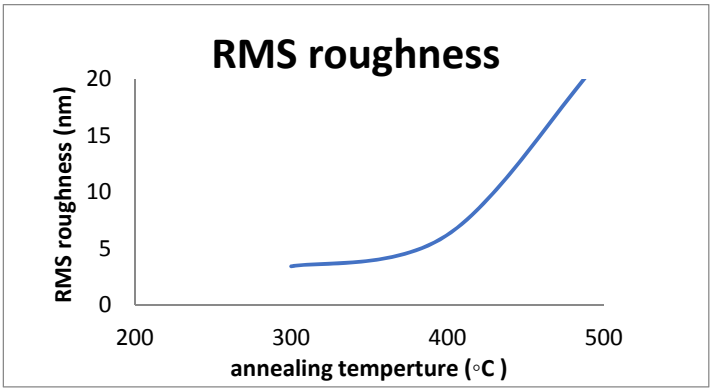

Fig.5: The RMS roughness of ZnO nanostructures at different annealing temperature.

Fourier Transform Infrared Spectroscopy (FTIR) measurements

Fig.6 displays FTIR spectra of metal oxide nanostructures synthesized from Zinc Nitrate dehydrate and 2.5M sodium hydroxide by hydrothermal method annealed at various temperatures (300, 400 and 500) °C. The peaks around 3431.48 cm^{-1} indicates O-H stretching mode related to hydroxyl group that assimilates presence of water molecules (H_2O) on the ZnO Nanostructures surface. The peak located at 2922 cm^{-1} referred to C-H stretching vibration of alkaline group. It can see the broad band observed in 1674 cm^{-1} belongs to C=N stretching vibration of oxime (=NOH) that attached to ZnO NSs during the synthesis. Peak located at1384.9 cm^{-1} was belong to C=O stretching vibration of Amides. The bands 1631.83 cm^{-1}, 1631.83 cm^{-1}, 1651.12 cm^{-1} were attributed to C=C stretching vibration of Alkaline group. Aromatic C=C stretch observed at 1504.53 cm^{-1}, 1546.96 cm^{-1}, 1462.09 cm^{-1} and 1465.95 cm^{-1} [19]. When increasing the annealing temperatures, size of ZnO nanoparticles increased and seen that contents of carboxylate groups in this sample run short as shown in Fig.7. The sharp peak observed in the range of (403.14 - 499.58) cm^{-1} was referred to vibrational phonon of ZnO Nanostructures. FT-IR peaks indicate the successful preparation of ZnO Nanostructures as shown in Table 4.

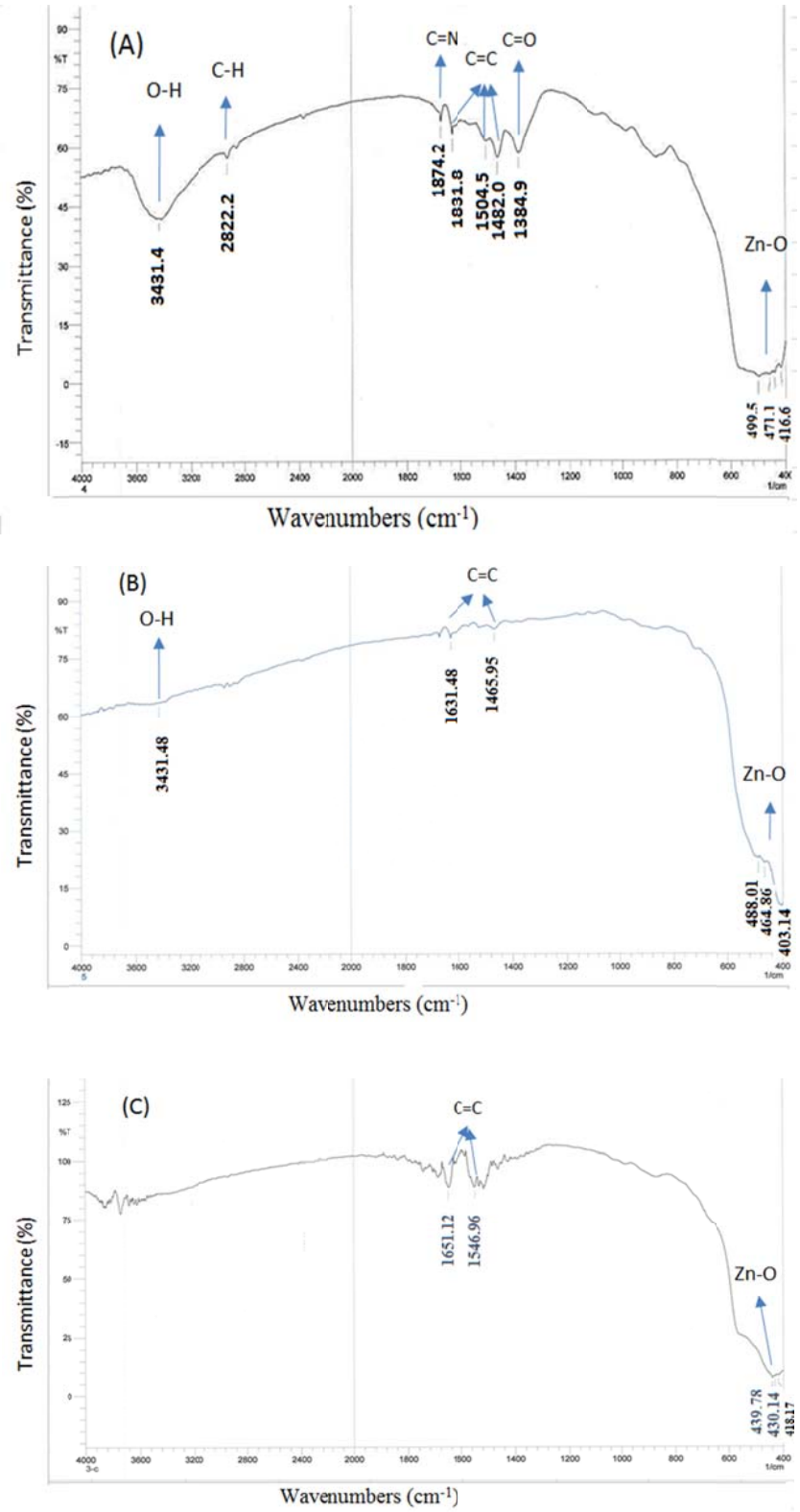

Fig.6: FTIR spectra of ZnO nanostructures prepared using 2.5 M NaOH annealed at a) 300 °C, B) 400 °C and C) 500 °C.

Table 4: FT-IR peaks of ZnO nanostructures.

Chemical bonds	The band locations cm-1		
	300 °C	400 °C	500 °C
O-H stretching mode of hydroxyl group	3431.48	3431.48	-
C-H stretching vibration of alkane groups	2922.25	-	-
C=N stretching vibration of oxime (=NOH)	1674.27	-	-
C=C stretching vibration of Alkene group	1631.83	1631.83	1651.12
Aromatic C=C stretch	1504.53 1462.09	1465.95	1546.96
C=O of stretching vibration of Amides	1384.9	-	-
Zn-O vibration	499.58 471.14 439.78 416.64	488.01 464.86 403.14	439.78 430.14 418.57

Optical properties

The optical absorbance of ZnO nanostructures annealed at various temperatures in the wavelength range (370-720) nm was measured. The different Ultra Violet-Visible absorption peaks among ZnO Nanostructures attributed to the difference that happens in their size and shape when utilized various annealing temperatures. Fig.7 displays optical absorption spectra of ZnO Nanostructures synthesized by using 2.5 M sodium hydroxide at different annealing temperatures (300, 400 and 500) °C. The increase of annealing temperature means increasing the particle size, changing the morphology and peak of absorbance wavelength becomes red shifted attributed to decreasing happen in quantum confinement as well as the absorbance spectra slightly decreased in the visible region as shown in Fig.7. Well, the absorbance of all samples decreases as the wavelength increases in the visible region. The obtained results agreed with previous literature [20].

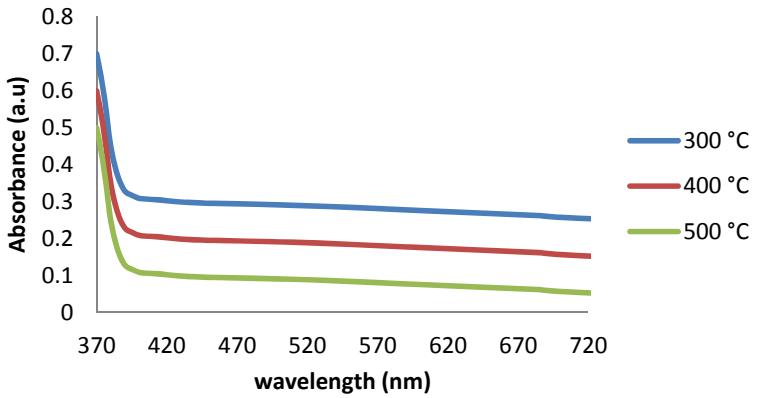

Fig.7: The optical absorption spectra of ZnO nanostructures prepared by hydrothermal method using 2.5 M NaOH with different annealing temperatures (300,400 and 500) °C

Optical band gap energy of ZnO nanostructures could be determined from optical absorption spectra as shown in Fig.8. Energy band gap can

be determined from plot of $(\alpha h\nu)^2$ vs. photon energy ($h\nu$). A value of energy gap (Eg) was recorded at Table 5 attributed to ZnO nanostructures annealed at different temperatures. Subsequently, Fig.8 indicates that decreased values of energy gap with increasing annealing temperatures because quantum confinement effect [21]. The quantum confinement leads to the decrease the E_g because number of orbitals increased participating in the formation of VB and CB through orbital overlap.

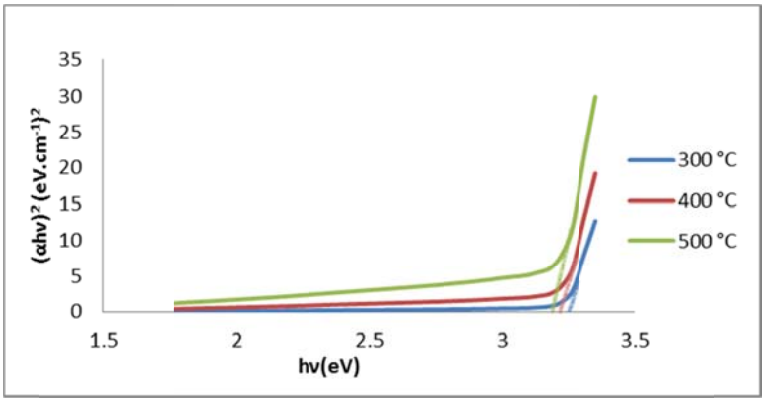

Fig. 8: Plot of (αhυ)2 vs. photon energy of ZnO nanostructures annealed at (300, 400 and 500) °C.

Table 5: The energy band gap (Eg) values of ZnO nanostructures at various annealing temperatures.

Annealing Temperature (°C)	Energy band gap (eV)
300 °C	3.22
400 °C	3.17
500 °C	3.12

Antibacterial activity test

Fig.9 exhibits the antibacterial activity of ZnO NSs prepared using (2.5M) NaOH concentration by hydrothermal method annealed at (300, 400 and 500) °C on gram positive (*S. aurous*) and gram-negative (*P.aeuruginosa*) Bacteria respectively. ZnO NSs revealed significant antibacterial activity on bacterium gram-positive than gram-negative bacteria as shown in Table 6 that good agreement with previous work [14, 22, 23]. The obtain results summarized that Zinc oxide NSs would be resisted growth of *S. aurous* bacteria due to the accumulation and adsorption of NPs in membrane outer or cytoplasm of bacterial cells and trigger Zn^{2+} release that penetrate into the cell and cause bacterial cell membrane disintegration resulting death of bacterial cells otherwise the *P.aeuruginosa* bacteria that may repeal the ZnO attachment onto the cell wall [24]. Many researchers suggest that the cell wall adsorption could follow its disintegration that means primary mechanism of toxicity [25, 26]. Adsorption of ZnO Nanoparticles leads to cell wall depolarization that would change negative charge of the wall turn out more permeable. Gram-positive (*S. aurous*) bacteria include a thick layer of peptidoglycan in their cell walls, whereas Gram negative bacteria (*P.aeuruginosa*) have a thin peptidoglycan layer having an additional outer membrane consisting of lipopolysaccharide [27]. ZnO

nanostructures (sample B1, B2, B3) cause disruption to bacterial membranes by production of reactive oxygen species such as hydroxyl radicals and superoxide. In this issue ZnO were strong depended on the nature of surface for various bacteria. Positively charged particles will attract negatively charged bacterial cells revealed electrostatic interaction that crucial for activity of nanoparticles bactericidal materials. These interactions may inhibit bacterial growth and produced the reactive oxygen species (ROS), ROS are species of oxygen considered as highly reactive and are produced during basic metabolism. Some ROS such hydroxyl radicals are negatively charge, that complain from difficult penetrate to the negative cell membrane that leads to cell death. Fig.10 showed the decreasing in the Growth of *S.aureus* inhibited by ZnO Nanostructures, Growth of gram positive and gram negative bacteria will increase with increasing annealing temperatures when increase crystal size of ZnO NSs. Antibacterial activity of ZnO NSs against (*P.aeuruginosa* and *S.aureus*) bacteria having small crystallite size was stronger than those with large crystallite size [28]. ZnO NSs of smaller sizes (as sample B1 in Table 6) may penetrate in bacterial membranes easily on account of their large interfacial area, thus optimizing their antibacterial efficiency [29]. Authors' study indicates that inhibitory efficacy of ZnO NSs is depending on size and chosen concentration. ZnO NSs have maximum antibacterial inhibition zone of 5mm in the concentration 1 mg in 5ml DMSO for S. aurous. In the present study, ZnO NSs have minimum inhibition zone of 3, 2, and 2 mm in the concentration 1 mg in 5ml DMSO for *P.aeuruginosa.* Other researchers investigated that ZnO shows high inhibition zone (29 and 19 mm) when utilized 10 mg/ml concentration against *S.aureus* [30]. The antibacterial activity of ZnO NSs on S. aurous and P.aeuruginosa bacteria became less efficient with increase the annealing temperature due to the crystallite size incensement.

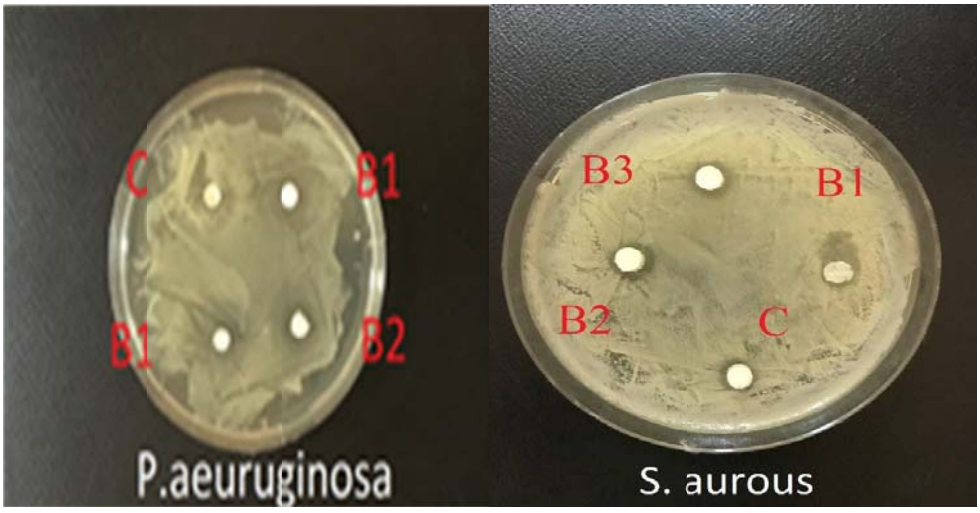

Fig.9: The antibacterial activity of ZnO Nanostructures, synthesized using 2.5 M NaOH and annealed at (300, 400 and 500) °C, on gram positive (S. aurous) and gram-negative (P.aeuruginosa).

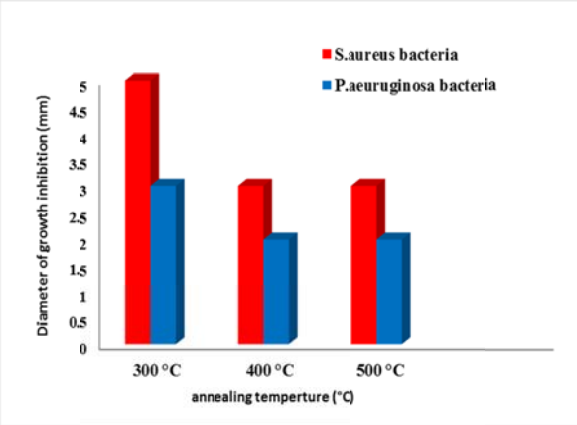

Fig.10: Growth of (S.aureus and P.aeuruginosa) bacteria inhibited by ZnO NSs.

Table 6: The antibacterial activity data of the sample.

1mg of ZnO in 5 ml DMSO for S. aurous					
annealing temperature	Sample name	mean (mm)	control zone (mm)	Diameter of inhibition (mm)	Concentration
300 °C	B1	14	9	5	25 µl
400 °C	B2	12	9	3	25 µl
500 °C	B3	12	9	3	25 µl
1mg of ZnO in 5 ml DMSO for P.aeuruginosa					
annealing temperature	Sample name	mean (mm)	control zone (mm)	Diameter of inhibition (mm)	Concentration
300 °C	B1	10	7	3	25 µl
400 °C	B2	9	7	2	25 µl
500 °C	B3	9	7	2	25 µl

Conclusions

Zinc oxide has been prepared using Zinc nitrate Hexahydrate and sodium hydroxide as a precursor via hydrothermal method to study the structural and morphological characterizations. The XRD analysis observed that the average crystallite size increased from 30.59 nm to 34.52 nm by increasing the annealing temperatures. The morphology, surface roughness, energy gap and grain size strongly depend on the annealing temperature. SEM images showed Nano-plate, compressed cylindrical pore and nanorods structures due to the difference in the annealing temperatures. The Average surface roughness of ZnO nanostructures increased from 3.96nm to 19.1 nm. The vibration phonon of ZnO nanostructures in the range of (403.14 - 499.58) cm^{-1} observed. The results of FTIR indicate to the successful preparation of ZnO Nanostructures. Optical absorption data were captured in the visible range. The gap energy value was (3.12-3.22) eV. The energy gap decreased with increasing of annealing temperatures due to the quantum confinements. ZnO Nanostructures showed stronger antibacterial activity towards gram-positive (*S. aurous*) bacterium than gram-negative (*P.aeuruginosa*) bacteria. In this study, antibacterial activity of ZnO NSs on *S. aurous* and *P.aeuruginosa* bacteria became less efficient with increase the annealing temperature due to the crystallite size incensement.

References

[1] A.M. Dalia, A.M. Mustafa, Journal of Nanoscience and Nanoengineering, 1, 4 (2015) 248-251.
[2] A. Geetha and J. Mallika, Journal of Science and Technology, 3, 2 (2015) 2349-5456.
[3] A. Azam, F. Ahmed, N. Arshi, M. Chaman, A.Naqvi, Inter. J of Theo. and App. Sci., 1, 2 (2009) 1-4.
[4] S.C. Pillai, J.M. Kelly, D.E. McCormack, R. Ramesh, Material Science Technology, 20 (2004) 964-968.
[5] S.C. Pillai, J.M. Kelly, D.E. McCormack, R. Ramesh, Advances in Applied Ceramics Adv. Appl. Ceram., 105, 3 (2006) 158-160.
[6] R. Georgekutty, M.K. Seery, S.C. Pillai, J Phys. Chem, C. 112, 35 (2008) 13563-13570.
[7] V. Gupta, R. Menon, K. Sreenivas, J. Appl. Phys., (2008) 55-58.
[8] N. Tang, J. Wang, H. Xu, H. Peng, C. Fan, Sci. China Ser. E-Technol. Sci., 52 (2009) 2200-2203.
[9] Z. Xu, H. Deng, J. Xie, Y. Li, Y. Li, X. Zu, S. Xue, J. Sol-Gel Sci Technol, 36 (2005) 223-226.
[10] P. Biswas, S. Kundu, P. Banerji, S. Bhunia, Sensors and Actuators B: Chemical, 178 (2013) 331-338.
[11] C. Changchun, Y. Benhai, L. Ping, L. JiangFeng, W. Lin, Journal of Ceramic Processing Research, 12, 4 (2011) 420-425.
[12] M. Vafaee, M. Sasani Ghamsari, Materials Letters, 61 (2007) 3265-3268.
[13] M. Premanathan, K. Karthikeyan, K. Jeyasubramanian, G. Manivannan, Nanomedicine: Nanotechnology Biology and Medicine, 7 (2011) 184-192.
[14] S. Getie, A. Belay, AR. Chandra Reddy, Z. Belay, J. Nanomed Nanotechnol, 0(0): 04 (2017) 2157-7439.
[15] A.R. Reddy, A. N. Mallika, K. S. Babu, International Journal of Mining, Metallurgy & Mechanical Engineering (IJMMME), 3, 2 (2015) 2320-4060.
[16] J. Mayekar, V. Dhar, S. Radha, International Journal of Research in Engineering and Technology, 3 (2014) 43-45.
[17] C.P. Rezende, J.B. Da Silva, N.D.S. Mohallem, Braz .J. Phys., 39 (2009) 248-251.
[18] P. F. Newhouse, Applied Physic Latters, 87 (2005) 108-112.
[19] A.E. Segneanu, I. Gozescu, A.Dabici, P. Sfirloaga, Z.Szabadai, "Organic compounds FT-IR spectroscopy", In Marco to Nano Spectroscopy, InTech, Romania, (2012).
[20] T. P. Kumar, S. Saravanakumar, K. Sankaranarayanan, J. of Elsevier Applied Surface Science, 257 (2011) 1923-1927.
[21] S. H. Sabeeh, R. H. Jassam, Journal of Results in Physics, 10 (2018) 212-216.
[22] Renata Dobrucka1, Jolanta Dlugaszewska, Mariusz Kaczmarek, Biomed Microdevices 20, 5 (2018) 1-13.
[23] J.S.Tawale, K.K. Dey, R.Pasricha K.N.Sood, A.K.Srivastav, J. of Elsevier Thin Solid Films, 519, 3 (2010) 1244-1247.
[24] J. Jiang, J. Pi and J. Cai, Bioinorganic Chemistry and Applications 3 (2018) 1-18.
[25] A. Thill, O. Zeyons, O. Spalla, F. Chauvat, J. Rose, M. Auffan, AM. Flank, Environ Sci. Technol., 40 (2006) 6151-6156.
[26] J.S. McQuillan, H.G. Infante, E. Stokes, A.M. Shaw, J. of Nanotoxicology, 6 (2012) 857-866.
[27] Y. N. Slavin, J. Asnis, U. O. Häfeli, H. Bach, Journal of Nanobiotechnology. 5 (2017) 15-65.
[28] W. Wu, T. Liu, H. He., Q. Sun X. Wu, X. Cao, J. Jin, Colloids and surfaces B: Bio interfaces, 167 (2018) 538-543.

[29] A. Sirelkhatim, S. Mahmud, A. Seeni, N. Haida, M. Kaus, L. Chuo, S.Khadijah, M. Bakhori, H. Hasan, D. Mohamad, Nano-Micro Letter, 7, 3 (2015) 219-242.

[30] Z. E. Karvani and P. Chehrazi, African Journal of Microbiology Research 5, 12 (2011) 1368-1373.